Moderate High Temperature is Beneficial or Detrimental Depending on Carbon Availability in the Green Alga *Chlamydomonas reinhardtii*

Ningning Zhang[1], Ming Xia[1], Catherine E. Bailey[1], Erin M. Mattoon[1,2], Ru Zhang[1,*]

[1]Donald Danforth Plant Science Center, St. Louis, Missouri 63132, USA;
[2]Plant and Microbial Biosciences Program, Division of Biology and Biomedical Sciences, Washington University in Saint Louis, St. Louis, MO 63130, USA.

Ningning Zhang: lucy.nnzhang@gmail.com
Ming Xia: celine.xia@wustl.edu, present address[2]
Catherine E. Bailey: cbailey@danforthcenter.org
Erin M. Mattoon: EMattoon@danforthcenter.org
Ru Zhang (rzhang@danforthcenter.org), corresponding author*

Running title: Algal responses to moderate high temperature

Highlight

We revealed the overlooked, dynamic effects of moderate high temperature in algae with different carbon availabilities and demonstrated the importance of carbon metabolism in thermotolerance of photosynthetic cells.

Abstract

High temperatures impair plant/algal growth and reduce food/biofuel production, but the underlying mechanisms remain elusive. The unicellular green alga *Chlamydomonas reinhardtii* is a superior model to study heat responses in photosynthetic cells due to its fast growth rate, many similarities in cellular processes to land plants, simple and sequenced genome, and ample genetic, genomic, and high-throughput tools. The interaction of heat responses with the availability of organic carbon sources is important for the algal biofuel/bioproduct industry but understudied. We cultivated Chlamydomonas wild-type cultures under highly controlled conditions in photobioreactors at control of 25°C,

moderate high temperature of 35°C, or acute high temperature of 40°C with and without constant organic carbon supply (acetate) for 1- or 4-days. Our results showed that moderate high temperature was beneficial to algal growth with constant acetate supply but detrimental without it. The overlooked and dynamic effects of 35°C can be explained by induced carbon metabolisms, including acetate uptake/assimilation, glyoxylate cycle, gluconeogenesis pathways, and glycolysis. Acute high temperature at 40°C for more than 2 days was lethal to algal cultures even with constant acetate supply. Our research provides insights to understand algal heat responses and help improve thermotolerance in photosynthetic cells.

Key words: moderate high temperature, acute high temperature, heat responses, *Chlamydomonas reinhardtii*, acetate, glyoxylate cycle, gluconeogenesis, glycolysis, photobioreactors

Abbreviations:

Photobioreactors (PBRs), Tris-acetate-phosphate (TAP) medium, Tris-phosphate (TP) medium

Introduction

Many biological processes in photosynthetic cells are sensitive to high temperatures (Mittler *et al.*, 2012; Schroda *et al.*, 2015; Janni *et al.*, 2020), including but not limited to photosynthesis (Sharkey and Zhang, 2010; Zhang *et al.*, 2022*a*), cell cycle (Hemme *et al.*, 2014; Zachleder *et al.*, 2019), membrane fluidity and Ca^{2+} channels (Saidi *et al.*, 2010; Gao *et al.*, 2012), DNA/RNA integrity (Su *et al.*, 2018; Han *et al.*, 2021), and protein stability (Rütgers *et al.*, 2017). Global warming increases the intensity, duration, and frequency of high temperatures in the field, reducing plant growth and food/biofuel production (Janni *et al.*, 2020). Nine of the ten hottest years on record occurred in the last 10 years from 2010 to 2021 due to human activities and the accumulation of greenhouse gases (NASA, Goddard Institute for Space Studies). A recent model revealed high temperature as the primary driver for yield loss in crops from 1981-2017 in US (Ortiz-Bobea *et al.*, 2019). Considering the increasing global temperature and human population,

it is imperative to improve plant thermotolerance and understand how photosynthetic cells respond to high temperatures.

High temperatures in the field have different intensities and durations. For many land plants or algae grown in moderate-temperature regions, moderate high temperatures refer to heat slightly above the optimal temperature for plant/algal growth (at or around 35ºC), while acute high temperatures refer to heat at or above 40ºC (Zhang *et al.*, 2022*a*). Moderate high temperatures are often long-lasting and frequent in nature with mild effects on photosynthetic cells, while acute high temperatures are often short-term but damaging. Most previous heat-stress experiments in plants used acute high temperatures at or above 40ºC (Balfagón *et al.*, 2019; Kim *et al.*, 2020; Ji *et al.*, 2021), likely due to the rapid onset and easily quantifiable phenotypes as compared to moderate high temperatures. Although the impact of moderate high temperatures in photosynthetic cells can be difficult to investigate due to comparatively mild phenotypes, moderate high temperatures are physiologically relevant stresses in field conditions and their frequent and long-lasting features could have significant impacts on agricultural yield (Delorge *et al.*, 2014; Anderson *et al.*, 2021). Global warming can further increase the frequency and duration of moderate high temperatures in nature. However, the effects of moderate high temperatures in photosynthetic cells are underexplored and often overlooked.

The unicellular green alga *Chlamydomonas reinhardtii* (Chlamydomonas throughout) is a superior model to study heat responses in photosynthetic cells (Schroda *et al.*, 2015). Chlamydomonas can grow in light under photoautotrophic conditions using photosynthesis and its photosynthetic structures are very similar to land plants (Minagawa and Tokutsu, 2015), presenting an excellent model to study heat effects on photosynthesis. Chlamydomonas can also grow with supplied organic carbon source (acetate) in light (mixotrophic) or dark (heterotrophic) conditions (Sasso *et al.*, 2018), providing a platform to study heat responses under different light/carbon conditions. Additionally, it has a haploid, sequenced, well-annotated, small genome (111 Mb, 17,741 protein-encoding genes) with simpler gene families and fewer gene duplications than land plants (Merchant *et al.*, 2007; Karpowicz *et al.*, 2011). Many land plants, like *Arabidopsis*

thaliana, have 21 or more copies of heat shock transcription factors (HSFs, the master regulators of heat responses) (Guo *et al.*, 2016). However, Chlamydomonas only has two HSFs, making it relatively easy to dissect the transcriptional regulation of heat responses in photosynthetic cells (Schulz-Raffelt *et al.*, 2007). Abundant transcriptome and proteome datasets under different conditions or from different cellular compartments are available in Chlamydomonas, facilitating systems-wide analysis and gene function prediction (Terashima *et al.*, 2011; Hemme *et al.*, 2014; Romero-Campero *et al.*, 2016; Salomé and Merchant, 2021; Zhang *et al.*, 2022*a*). Furthermore, several well-established gene editing and cloning tools are available in Chlamydomonas (Shimogawara *et al.*, 1998; Greiner *et al.*, 2017; Crozet *et al.*, 2018; Wang *et al.*, 2019; Dhokane *et al.*, 2020; Emrich-Mills *et al.*, 2021). A genome-saturating, mapped, indexed, Chlamydomonas insertional mutant library is available for reverse/forward genetic screens and functional genomics (Li *et al.*, 2016, 2019). Genome-wide screens for heat-sensitive Chlamydomonas mutants have been conducted to identify novel genes with putative roles in thermotolerance in photosynthetic cells (Fauser *et al.*, 2022; Mattoon *et al.*, 2022).

Algae have great potential for production of biofuels and bioproducts (Scranton *et al.*, 2015; Mathimani and Pugazhendhi, 2019). However, how algal cells respond to high temperatures is under-investigated as compared to land plants (Schroda *et al.*, 2015). Outdoor algal ponds frequently experience moderate high temperatures around 35°C during summer time (Mata *et al.*, 2010), but the effects of moderate high temperatures on algal growth have been overlooked. Previously published algal heat treatments were often conducted in flasks with incubation in pre-warmed water baths at or above 42°C with sharp temperature switches and without control of nutrients (Hemme *et al.*, 2014; Rütgers *et al.*, 2017)). While previous research was highly valuable to understand algal heat responses, high temperatures in the field or outdoor ponds often increase gradually. Heating speeds affect heat responses in plants (Mittler *et al.*, 2012) and rapid increases to high temperatures largely reduce algal viability (Zhang *et al.*, 2022*a*). Acute high temperatures at or above 40°C inhibit algal cell division (Mühlhaus *et al.*, 2011*b*; Hemme *et al.*, 2014; Zachleder *et al.*, 2019; Ivanov *et al.*, 2021/5), while moderate high temperature at 35°C only transiently inhibits cell division during the first 4-8 hour (h) heat

(Zhang *et al.*, 2022*a*). Thus, conducting long-term experiments at moderate high temperatures in flasks can result in overgrown cultures, nutrient depletion, and light limitation, complicating data interpretation.

Consequently, it is advantageous to investigate algal heat responses under highly-controlled conditions in photobioreactors (PBRs) (Zhang *et al.*, 2022*a*; Mattoon *et al.*, 2022), which have several evident strengths: (1) controlled heating to mimic the heating speed in nature; (2) precise temperature regulation with a sterile temperature probe inside each algal culture; (3) the availability of turbidostatic control based on defined parameters (e.g., chlorophyll contents) to enable frequent culture dilutions using fresh medium; (4) precisely controlled cultivation condition, including temperature, light, nutrient, and air agitation, allowing for reproducible experiments; (5) automatic recording of culture status every minute, e.g. growth conditions, optical densities, enabling quantitative growth rate measurements; (6) being able to simulate nutrient depletion by turning off the turbidostatic control to investigate how nutrient availability affects algal heat responses. Utilization of PBRs for algal cultivation and heat treatments can largely reduce compounding effects during high temperature treatments and improve our understanding of algal heat responses.

Recently, we conducted systems-wide analyses in wild-type (WT) Chlamydomonas cultures during and after 24-h heat of 35^{o}C and 40^{o}C in PBRs with constant nutrient supply and light in acetate-containing medium (mixotrophic condition) (Zhang *et al.*, 2022*a*). Our results showed that 40^{o}C inhibited algal growth while 35^{o}C increased algal growth. The growth inhibition at 40^{o}C could be explained by reduced photosynthesis, impaired respiration, and cell cycle arrest, while these cell parameters had minor changes in algal cultures treated by 35^{o}C. Our proteomics data indicated that several proteins involved in acetate uptake/assimilation, glyoxylate cycle, and gluconeogenesis were up-regulated during 35^{o}C (Zhang *et al.*, 2022*a*). Chlamydomonas uptakes acetate and feeds it into the glyoxylate cycle and gluconeogenesis for starch biosynthesis (Johnson and Alric, 2012, 2013). The main function of glyoxylate cycle is to allow growth when glucose is unavailable and two-carbon compounds, e.g., acetate, are the organic carbon source;

glyoxylate cycle is a shunt of the tricarboxylic acid (TCA) cycle in mitochondria but without CO_2 releases to allow for the anabolism of simple carbon compounds in gluconeogenesis, a process to make sugars, namely glucose (Johnson and Alric, 2012; Chew *et al.*, 2019; Walker *et al.*, 2021).

We hypothesized that the increased growth in Chlamydomonas at 35°C with constant acetate supply was attributable to up-regulated acetate metabolisms, including the pathways mentioned above. The majority of published high temperature research in Chlamydomonas has been conducted in acetate-containing medium (Voß *et al.*, 2010; Mühlhaus *et al.*, 2011*a*; Hemme *et al.*, 2014; Rütgers *et al.*, 2017; Zhang *et al.*, 2022*a*), but the interface between acetate supply and algal heat responses is understudied. To validate our hypothesis and address these unknown questions, we cultivated the same Chlamydomonas WT strain in PBRs as before but heated the cultures at 35°C or 40°C with and without constant acetate supply for 1 or 4 days. Our results revealed the overlooked effects of moderate high temperature of 35°C on algal growth which can be beneficial or detrimental based on acetate availability. Acute high temperature at 40°C is lethal to algal cultures, even with constant acetate supply. Our research provided insights to understand algal heat responses and help improve thermotolerance in photosynthetic cells.

Materials and methods

Algal cultivation

Chlamydomonas reinhardtii wild-type strain CC-1690 (also called *21gr*, mating type plus) (Pröschold *et al.*, 2005; Zhang *et al.*, 2022*b*; Sager, 1955-7) was purchased from the Chlamydomonas resource center and used in all experiments. Algal cultures were grown in Tris-acetate-phosphate (TAP, with acetate) or Tris-phosphate (TP, without acetate) medium with revised trace elements (Kropat *et al.*, 2011) in 400 mL photobioreactors (PBRs) (Photon System Instruments, FMT 150/400-RB) as described before (Zhang *et al.*, 2022*a*). Cultures were illuminated with constant 100 µmol photons m^{-2} s^{-1} light (red: blue, 1:1 ratio), and agitated by bubbling with filtered air at a flow rate of 1 L min^{-1}. Algal

cultures with targeted cell density around 2 x10^6 cells mL^{-1} (~4.0 µg mL^{-1} chlorophyll content) were maintained at 25°C for 4 days with constant nutrient supply through a turbidostatic mode before different temperature treatments. The turbidostatic mode was controlled by OD_{680} (optical density at 680 nm), which is proportional to chlorophyll contents (µg mL^{-1}) and was monitored once per min automatically. When OD_{680} increased to a maximum value slightly above the target value (for target cell density) due to algal growth, OD_{680} signaled the control computer to turn on a turbidostatic pump to add fresh medium to dilute the culture until a minimum OD_{680} slightly below the target value was reached, then the turbidostatic pump was turned off automatically. Because of the small OD range we used, the PBR cultures had exponential growth between dilution events through the turbidostatic mode with constant nutrient supply (Fig. 1A). The OD_{680} data during exponential growth phases in between dilution events was $\log_2$ transformed, and the relative growth rate was calculated using the slope of $\log_2(OD_{680})$. The relative growth rate is an inverse of the doubling time of an algal culture. For the treatments without constant nutrient supply, the turbidostatic pumps were turned off after PBR cultures reached steady growth and at the start of different temperature treatments.

High temperature treatments in PBRs

After algal cultures in PBRs reached steady growth with turbidostatic control at 25°C for 4 days, PBR temperatures were increased to moderate or acute high temperatures (35°C or 40°C in different PBRs) for the indicated duration with indicated nutrient conditions. PBR temperatures were changed from 25°C to 35°C or 40°C gradually over the course of 30 min with controlled heating speeds. PBR cultures grown under constant 25°C with the same nutrient status and treatment duration served as controls. Algal cultures were harvested from PBRs at different time points during different treatments for various measurements.

Algal biomass quantification

Algal cultures (90 mL) were harvested from PBRs, centrifuged to remove supernatants, flash frozen in liquid nitrogen, then stored in a -80°C freezer until analysis. Algal cell

pellets were freeze dried for 24 h over liquid nitrogen. The remaining algal dry biomass were weighted and quantified.

Acetate quantification assay

Algal cultures were harvested from PBRs (2 mL) and centrifuged to collect 500 µL top clear supernatants to a new tube. The supernatant was stored in a -80°C freezer until analysis. The acetate content in the supernatant was quantified using the Acetate Colorimetric Assay Kit (Sigma, Cat No. MAK086) according to manufacture instructions.

RT-qPCR analysis

PBR cultures of 2 mL were pelleted with Tween-20 (0.005%, v/v) by centrifugation at 11,363 x g and 4°C for 2 min, followed by supernatant removal. The cell pellet was flash frozen in liquid nitrogen and then stored in a -80°C freezer until processing. RNA extraction and RT-qPCR analysis were performed as before with minor modifications (Zhang *et al.*, 2022*a*). Total RNA was extracted with TRIzol reagent (Thermo Fisher Scientific, Cat No. 15596026), digested on-column with RNase-free DNase (Qiagen, Cat No. 79256), purified by RNeasy mini-column (Qiagen, Cat No. 74106), and quantified with Qubit™ RNA BR Assay Kit, (Life technology, Cat No. Q10210). Total 0.4 µg RNA was reverse transcribed with oligo dT primers using SuperScript® III First-Strand Synthesis System (Life technology, Cat No. 18080-051) following manufacturer instructions. Quantitative real-time PCR (RT-qPCR) analysis was performed using a CFX384 Real-Time System (C 1000 Touch Thermal Cycler, Bio-Rad, Hercules, California) using SensiFAST SYBR No-ROS kit (Bioline, BIO-98020) following this set-up: (1) 95°C (2 min); (2) 40 cycles of 95°C (5 s), 60°C (10 s), and 72°C (15 s); (3) final melt curve at 60°C (5 s), followed by continuous temperature ramping from 60°C to 99°C at a rate of 0.5°C s^{-1}. Melting curves and qPCR products were tested to ensure there were no primer dimers or unspecific PCR products. All RT-qPCR products were sequenced for confirmation. Primers and gene IDs for RT-qPCR were included in Supplementary Table S1. *CBLP* (*β-subunit-like polypeptide*, Cre06.g278222), (Schloss, 1990; Xie *et al.*, 2013) and *EIF1A* (*Eukaryotic translation initiation factor 1A,* Cre02.g103550) (Strenkert *et al.*, 2019) had stable expression among all time points, and were used as reference genes for RT-qPCR

248 normalization. The relative gene expressions were calculated relative to the pre-heat time
249 point by using the $2^{-\Delta\Delta CT}$ method (Livak and Schmittgen, 2001; Hellemans *et al.*, 2007;
250 Remans *et al.*, 2014). Three biological replicates were included for each time point and
251 treatment.

252

253 **Cell imaging using light microscopy**

254 Chlamydomonas cultures harvested at select time points with different temperature
255 treatments were fixed with 0.2% glutaraldehyde (VWR, Cat No. 76177-346). Algal cells
256 were imaged with a Leica DMI6000 B microscope and a 63x (NA1.4) oil-immersion
257 objective.

258

259 **Chlorophyll quantification**

260 Chlorophyll contents in algal cells were quantified as before (Zhang *et al.*, 2022*b*,*a*). PBR
261 cultures of 1 mL were harvested in 1.5-mL tubes with 2.5 µL 2% Tween20 (Sigma, P9416-
262 100ML, to help cell pelleting), and centrifuged at 18,407 g at 4°C. After removing
263 supernatant, cell pellets were stored in a -80°C freezer until quantification. Later, cell
264 pellets were thawed, resuspended in 1 mL of HPLC grade methanol (100%, Sigma,
265 34860-4L-R), vortexed for 1 min, incubated in the dark at 4°C for 5 min, and centrifuged
266 at 15,000 g at 4°C for 5 min. Supernatant was pipetted out to a two-sided disposable
267 plastic cuvettes (VWR, 97000-586) for chlorophyll (Chl) quantification at 652 and 665 nm
268 in a spectrophotometer (IMPLEN Nonophotometer P300) using the following equations:
269 Chl a + Chl b = $22.12*A_{652} + 2.71*A_{665}$ (in µg mL^{-1} algal cultures) (Porra *et al.*, 1989).
270 Chlorophyll concentrations were also normalized to cell densities (Chl pg $cell^{-1}$) or algal
271 cell volume (Chl pg μm^{-3}). Cell density and mean cell volume were measured using a
272 Coulter Counter (Multisizer 3, Beckman Counter, Brea, CA).

273

274 **Differential expression heatmaps**

275 Our previously published RNA-seq and proteomics data (Zhang *et al.*, 2022*a*) were used
276 to identify the expression patterns of genes of interest. Heatmaps were generated using

the R package pheatmap (version 1.0.12. https://CRAN.R-project.org/package=pheatmap).

Results

To investigate how the availability of organic carbon source affected algal heat responses, we first cultivated WT Chlamydomonas cells (CC-1690, *21gr*) in PBRs in Tris-acetate-phosphate (TAP, acetate as carbon source) medium at 25ºC with constant nutrient supply through turbidostatic control (providing frequent fresh medium and culture dilution) (Fig. 1A, B). After algal cultures reached steady growth rates in PBRs, the turbidostatic control was turned off and cultures were switched to 35ºC, or 40ºC, or stayed at 25ºC for 24 h without constant acetate supply. Algal cultures were harvested at different time points to analyze cell physiologies, transcripts, and biomass (Fig. 1B). Algal dry biomass quantification showed that cultures treated with 35ºC had increased biomass at 8-h heat but decreased biomass at 24-h heat as compared to 25ºC (Fig. 1C). Acetate quantification in the supernatant of algal cultures indicated that 35ºC-treated cultures had increased acetate consumption and depleted acetate faster than 25ºC or 40ºC (Fig. 1D).

We suspected the transiently increased and then decreased algal biomass in 35ºC-treated cultures may be due to increased acetate uptake/usage followed by acetate starvation without constant acetate supply (Fig. 1). Chlamydomonas uptakes acetate and feeds it into the glyoxylate cycle and gluconeogenesis for starch biosynthesis (Johnson and Alric, 2012, 2013) (Fig. 2A). To verify this hypothesis, we investigated transcripts involved in the glyoxylate and gluconeogenesis cycles (Fig. 2A-E). ICL1 and MAS1 are key enzymes involved in glyoxylate cycle; PCK1 and FBP1 are key enzymes involved in gluconeogenesis pathways (Johnson and Alric, 2012, 2013; Plancke *et al.*, 2014) (Fig. 2A). The relative expression levels of three of these four transcripts (except FBP1) were significantly down-regulated at 24-h of constant 25ºC without constant acetate supply as compared to the pre-heat time point (with constant acetate supply), consistent with the acetate-depleting condition (Fig. 2B-E). However, the expression levels of three of these four genes (except for FBP1) were significantly higher in algal cultures treated with 24-h 35ºC than 25ºC. Although only the relative expression levels of *MAS1* at a few limited

time points were significantly reduced at 40°C than 25°C, the expression levels of *ICL1*, *MAS1*, *PCK1* were significantly reduced in algal cultures treated with 40°C than 35°C for almost all time points during the 24-h heating, suggesting reduced glyoxylate cycle and gluconeogenesis pathways in 40°C-treated cultures (Fig. 2B-E). Using our previously published transcriptomes and proteomes from algal cultures with constant acetate supply and turbidostatic control (grown in the same PBRs and acetate-containing medium), we confirmed the largely down-regulated transcripts related to glyoxylate cycle and gluconeogenesis in 40°C-treated cultures and up-regulated proteins related to these pathways in 35°C-treated cultures (Fig. F, G). These results suggested glyoxylate cycle and gluconeogenesis increased under 35°C heat but decreased under 40°C heat.

Without constant acetate supply, 35°C and 40°C affected algal cell physiologies differently. 35°C-treated algal cells had transiently increased then decreased cell size while 40°C-treated algal cells had steadily increased cell size due to heat-inhibited cell division (Fig. 3). We quantified the cellular parameters before and during heat and compared the results with and without constant acetate supply (Fig. 4). Without constant acetate supply and turbidostatic dilution, cell density increased steadily during 25°C and 35°C but had little change during 40°C (Fig. 4A), consistent with cell cycle arrest under 40°C (Zhang *et al.*, 2022*a*). The cell density was significantly lower at 35°C than 25°C at 8-h and 24-h time points (Fig. 4A). The mean cell volume was constant during 25°C treatment, transiently increased under 35°C, and was close to 3X pre-heat volume at the end of 40°C heat, in agreement with our microscopic images (Fig. 3). Chlorophyll content per culture volume (mL) had no significant differences between 25°C and 40°C but was significantly higher at 8-h of 35°C than 25°C (Fig. 4C), consistent with the increased biomass at the 8-h of 35°C (Fig. 1C). Chlorophyll content normalized to cell density revealed constant chlorophyll per cell during 25°C, but transiently and constantly increased cellular chlorophyll during 35°C and 40°C, respectively (Fig. 4D). Chlorophyll content normalized to cell volume showed the increased cellular chlorophyll during 40°C and 35°C cannot be completely explained by increased cell volume (Fig. 4E).

Based on our previously published data, we summarized cell parameters in algal cultures grown in the same PBRs but with constant acetate supply through turbidostatic control (Zhang *et al.*, 2022*a*) (Fig. 4F-J). Cell parameters at different time points during 25°C had little or no changes as compared to the pre-heat time points, demonstrating the effectiveness of the turbidostatic control with constant acetate supply. The changes of cell volume and chlorophyll content per cell during 35°C and 40°C had the similar trends with and without constant acetate supply, but the increase of these parameters was larger under 40°C in cultures with constant acetate supply than without (Fig. 4B, D, G, I). This was supported by the fold change of cell parameters by comparing the data with and without constant acetate supply (Fig. 4K-O).

In addition to the cellular parameters mentioned above using time-course harvesting, we next utilized non-disruptive methods to quantify algal growth under different temperatures without constant acetate supply. OD_{680} (optical density at 680 nm) monitors chlorophyll content per mL culture (Chapman *et al.*, 2015; Xiao *et al.*, 2015; Young *et al.*, 2022). OD_{750} (optical density at 750 nm) monitors light scattering and is thought to be proportional to cell density (Chioccioli *et al.*, 2014; Young *et al.*, 2022). Our PBRs have OD_{680} and OD_{720} settings, but no OD_{750}. However, OD_{720} serves as a proximity for OD_{750} for light scattering. Thus, we investigated the dynamic changes of OD_{680} and OD_{720} relative to chlorophyll content and cell density before and during heat treatments in medium starting with acetate but without constant acetate supply (Fig. 5). The change of OD_{680} (Fig. 5A) mimicked the change of chlorophyll content per mL algal culture for all three temperature treatments (Fig. 4C) while the change of OD_{720} (Fig. 5B) mimicked the change of cell density for 25°C and 35°C but not 40°C (Fig. 4A). Combining all data from different temperature treatments and time points, both OD_{680} and OD_{720} were linearly proportional to chlorophyll content per mL algal culture (Fig. 5C, D), but they were much less proportional to cell density, with evident deviations at the high OD range (Fig. 5E, F) and even lower correlations at the low OD range (Fig. 5G, H). Our results showed that OD_{680} and OD_{720} can be used to accurately estimate chlorophyll accumulation in algal cultures with different heat treatments, thus they can be used to estimate algal relative growth rates based on chlorophyll accumulation during an exponential growth phase

between dilution events with turbidostatic control in PBRs (Zhang *et al.*, 2022*a*) (See methods for details). The relative growth rates calculated from both OD_{680} and OD_{720} yielded similar results. Because OD_{680} had larger values and higher signal/noise ratios than OD_{720}, we used OD_{680} to estimate relative growth rates of PBR cultures over several days with turbidostatic controls and constant acetate supply to investigate how 35°C and 40°C affected algal heat responses in long-term (Fig. 6). This research goal could not be achieved without turbidostatic controls because acetate in the TAP medium was fully depleted in 24 h during all three temperature treatments of 25°C, 35°C and 40°C without constant acetate supply (Fig. 1D).

To investigate the effects of acetate on long-term heating, after algal cultures reached steady growth at 25°C in PBRs with turbidostatic control, we conducted all three temperature treatments with continuously turbidostatic control and constant acetate supply for 4 days (Fig. 6). Without heat treatments, algal growth rates and cell parameters stayed constant at 25°C, demonstrating the effectiveness of our turbidostatic control for algal growth (Fig. 6). At 35°C with constant acetate supply, the relative growth rates increased first, but the increase was reduced to a smaller degree after 2-day heating at 35°C and stabilized thereafter (Fig. 6A). At 40°C, the relative growth rates decreased steadily, and the cultures died after 2-day heating at 40°C, suggesting algal cells could not acclimate to long-term constant 40°C, even with constant acetate supply. Cell densities and chlorophyll per cell of 35°C-treated cultures had cycling pattern, with approximately 24-h period, which diminished at the end of 4-day heating (Fig. 6B, E). Cells treated with 40°C had more than 4-fold increase of cell volume as compared to the pre-heat condition, followed by reduced cellular chlorophyll and cell death (Fig. 6C-F). The turbidostatic mode by OD_{680} tightly controlled the chlorophyll contents in unit of ug per mL culture in PBRs during the treatments of 25°C and 35°C (Fig. 6D), but not 40°C due to the cell cycle arrest and overwhelmingly increased chlorophyll per cell, and eventually cell death under 40°C (Fig. 6B and E).

In algal cultures with constant medium supply via turbidostatic control but without acetate, the relative growth rates decreased at 35°C (Fig. 7A), in contrast to the increased growth

rates under 35°C with constant acetate supply (Fig. 7B). This supports our hypothesis that the increased growth during 35°C with constant acetate supply (Fig. 6A) is due to increased carbon (acetate) metabolisms: acetate uptake/assimilation, glyoxylate cycle, and gluconeogenesis (Fig. 2A).

Discussion

By performing algal cultivation under highly controlled conditions in PBRs with and without a constant organic carbon source, acetate, we investigated how the availability of organic carbon supply affected the growth of Chlamydomonas under moderate (35°C) and acuate high temperatures (40°C).

Heat of 35°C was beneficial or detrimental depending on carbon availability

Moderate high temperature of 35°C increased algal growth rates with constant acetate supply (Fig. 6A) (Zhang *et al.*, 2022*a*). Without acetate in photoautotrophic medium, heat of 35°C decreased agal growth rates (Fig. 7), confirming the important role of the organic carbon source, acetate, in heat tolerance. The increased heat tolerance to 35°C with acetate is not strain-dependent because the acetate effects were similar in two different algal strains: CC-1690 (this study) and CC-5325 (Mattoon *et al.*, 2022). In medium starting with acetate but without constant acetate supply, algal biomass increased first but then decreased at 35°C compared to 25°C, which can be explained by increased acetate uptake/usage initially followed by acetate depletion/starvation by the end of the 24-h 35°C treatments (Fig. 1C, D). In medium starting with acetate but without turbidostatic control and frequent dilutions (Fig. 1B), other nutrients, e.g., nitrogen may also be reduced or depleted in 24-h of treatments, but our results strongly pointed to the effects of acetate on algal heat responses (Fig. 7), which is the focus of our research.

Chlamydomonas uptakes acetate and feeds it into the glyoxylate cycle and gluconeogenesis for starch biosynthesis and starch is broken down through glycolysis to make cellular energy (Johnson and Alric, 2012, 2013) (Fig. 2A).The dynamic effects of 35°C on algal growth under different acetate conditions can be explained by the 35°C-induced carbon metabolisms, including but not limited to the up-regulation of acetate

uptake/assimilation, glyoxylate cycle and gluconeogenesis pathways, and glycolysis (Fig. 1D, 2) (Zhang *et al.*, 2022*a*). Our previous proteomic data showed significantly up-regulated proteins involved in these carbon metabolism pathways mentioned above (Zhang *et al.*, 2022*a*). Energy produced from glycolysis can be used for energy-requiring cellular activities to increase thermotolerance (Olas *et al.*, 2021), e.g., production of heat shock proteins and repair pathways related to photosynthesis (Murata and Nishiyama, 2018; Bourgine and Guihur, 2021). Pyruvate kinase catalyzes the final step of glycolysis and it converts phosphoenolpyruvate and one ADP to pyruvate and one ATP (Baud *et al.*, 2007; Wulfert *et al.*, 2020). Chlamydomonas mutants deficient in pyruvate kinase were heat-sensitive under 35°C in acetate-containing medium (Mattoon *et al.*, 2022), supporting the important roles of glycolysis in thermotolerance of 35°C. Although ATP production mainly comes from mitochondrial respiration, the ATP production from glycolysis can be important under stressful conditions where energy availability is limited (van Dongen *et al.*, 2011). Under low oxygen conditions, plants increase activity of pyruvate kinases to produce more ATP (van Dongen *et al.*, 2011). Heat-treated barley leaves utilized glycolysis as an alternative energy source for thermotolerance based on proteomics analysis (Rollins *et al.*, 2013), consistent with our previous proteomic results in Chlamydomonas (Zhang *et al.*, 2022*a*).

Additionally, acetate may protect photosynthesis from heat-induced photoinhibition. Acetate is proposed to protect photosystem II (PSII) against photoinhibition by replacing the bicarbonate associated to the non-heme iron at the acceptor side of PSII, changing the environment of plastoquinone, and affecting PSII charge recombination (Roach *et al.*, 2013). Chlamydomonas grown in acetate-containing medium produced less singlet O_2 (one kind of reactive oxygen species, ROS) than those grown in non-acetate-containing, photoautotrophic medium (Roach *et al.*, 2013). Furthermore, experimental and modeling analysis suggested that acetate promoted cyclic electron flow (CEF) around photosystem I (PSI); reducing equivalents produced during the acetate metabolism reduce plastoquinone pools and increase CEF activity (Johnson and Alric, 2012; Lucker and Kramer, 2013; Chapman *et al.*, 2015). CEF cycles photosynthetic electrons around PSI, producing only ATP but no NADPH and providing extra ATP needed for photosynthesis

and other cellular activities (Munekage *et al.*, 2004; Baker *et al.*, 2007). CEF balances the ATP/NADPH ratio, contributes to the generation of transthylakoid proton motive force, and protects both PSI and PSII from photo-oxidative damage (Johnson, 2011; Yamori and Shikanai, 2016). The increased acetate uptake under 35ºC (Fig. 1D) was coupled with induced CEF activity measured by P700 oxidation/reduction in Chlamydomonas (Zhang *et al.*, 2022*a*).

On the other side, acerate is reported to suppress the activity of photosynthesis (Heifetz *et al.*, 2000; Chapman *et al.*, 2015). In the presence of acetate, photosynthesis is less important for algal growth than in photoautotrophic conditions without acetate. Photosynthesis is one of the most heat sensitive functions in plants (Sharkey, 2005; Sharkey and Zhang, 2010) and is also the major source of ROS when photosynthetic activity is compromised by heat (Pospíšil, 2016; Qin-Di *et al.*, 2021; Niemeyer *et al.*, 2021). Although moderate high temperature of 35ºC did not affect thylakoid structures or PSII activities significantly, the increased non-photochemical quenching (NPQ, photoprotection pathway) (Rochaix, 2014; Erickson *et al.*, 2015) in 35ºC-treated Chlamydomonas cells still suggested non-optimal or compromised photosynthesis at 35ºC (Zhang *et al.*, 2022*a*). The suppression of photosynthetic activities by acetate may alleviate the heat-induced damages to photosynthesis and reduce ROS production at 35ºC.

With constant acetate supply, 35ºC is beneficial, increasing carbon metabolisms and energy production, thus improving thermotolerance and growth (Fig. 8). If algal cells can be cultivated under sterile conditions with constant organic carbon supply, 35ºC could be used to promote algal growth and increase biofuel/bioproduct generation under mixotrophic conditions in light. Culture temperature of 35ºC in closed, outdoor algal ponds may not be difficult to reach with natural sunlight heating in the summertime of the moderate climate regions and most time of the tropical regions.

Without constant acetate supply, 35ºC is detrimental. The 35ºC-induced up-regulation carbon metabolism seem independent of acetate availability, but rather resulted from a

high-temperature effect (Fig. 2). Without constant acetate supply, when acetate was fully depleted after 24-h growth, transcripts involved in glyoxylate cycle and gluconeogenesis pathways were down-regulated in the 25°C control culture but up-regulated in the 35°C-treated culture (Fig. 2B-E). The 35°C treatment elevated carbon metabolism without sufficient carbon input which may deplete cellular carbon reserves. This was not sustainable in the long term and eventually reduced biomass accumulation (Fig. 1C). Such effects of 35°C can particularly compromise the yields of outdoor algal ponds because they usually do not contain carbon sources but frequently experience moderate high temperatures (Mata *et al.*, 2010; El-Sheekh *et al.*, 2019). The up-regulated carbon metabolism under moderate high temperatures may also occur in land plants, especially in sink tissues (e.g., roots) or mixotrophic tissues (e.g., developing green seeds) (Koley *et al.*, 2022). Heat-induced glyoxylate cycle, gluconeogenesis, and glycolysis have been reported in plants (Rollins *et al.*, 2013; Zhang *et al.*, 2013; Aprile *et al.*, 2013). Carbon metabolism and sugar availability were shown to be essential for heat tolerance in Arabidopsis (Olas *et al.*, 2021). Without sufficient carbon supply from source tissues (e.g., leaves), long-term moderate high temperatures may result in significant loss of plant yield (Li *et al.*, 2015; Qin-Di *et al.*, 2021). Arabidopsis seedlings treated with 5-day heat at 35°C had reduced growth and viability (Song *et al.*, 2021).

With constant acetate supply, heat at 35°C transiently arrested the cell cycle, which fully recovered after 8 h at 35°C, based on DNA content analysis and the expression pattern of cell cycle genes (Zhang *et al.*, 2022*a*). Additionally, our previous results revealed partial culture synchronization induced by 35°C (Zhang *et al.*, 2022*a*). Our pre-heat PBR cultures were grown asynchronously under constant light and temperature (25°C) with turbidostatic control and frequent medium supply so the circadian rhythm of the cultures should be none or minimal without heat treatments, as evidenced by the steady relative growth rates and cell parameters under constant 25°C (Fig. 6). The cycling pattern of cell densities and chlorophyll per cell during 4-day 35°C heat may be related to the 35°C-induced culture synchronization (Fig. 6B, E). Synchronized cultures at 35°C grew up between two sequential dilution events as evidenced by increased chlorophyll per cell (Fig. 6E). The speed of increase in chlorophyll per cell (or the relative growth rates) was

faster at 35°C than 25°C (Fig. 6A). The turbidostatic dilution is controlled by OD_{680}, which is proportional to chlorophyll per mL culture (Fig. 5, 6D). Thus, the trend of chlorophyll per cell was opposite to that of cell density, with the maximum of the chlorophyll per cell overlapping with the minimum of cell density under 35°C (Fig. 6B, E).

The gradually reduced cycling pattern of the chlorophyll per cell and cell density during 4-day of 35°C may be related to the heat effects on circadian clock (Fig. 6B, E). High temperatures impact the circadian clock in plants (Kusakina *et al.*, 2014; Gil and Park, 2019; Mody *et al.*, 2020). Light and temperatures are the two strongest environmental signals that can entrain the plant biological clock (the period of the clock is synchronized to the period of the entraining signal); however, the mechanisms of temperature entrainment is much less understood as compared to light entrainment (Gil and Park, 2019). How temperatures affect circadian clock in algal cells is largely underexplored but an RNA-binding protein CHLAMY1 was reported to be involved in the regulation and temperature entrainment of circadian clock in Chlamydomonas (Iliev *et al.*, 2006; Voytsekh *et al.*, 2008). The gradually diminished cycling pattern of the chlorophyll per cell and cell density was probably because the onset of heat at 35°C provided a signal to entrain the circadian clock of the asynchronized pre-heat cultures, but the entrainment became less effective over time under the constant 35°C which lacked a circadian rhythm of heat treatments.

Heat of 40°C was detrimental to algal cells even with constant acetate supply

Unlike the transient effects of moderate high temperature at 35°C, acute high temperatures at or above 40°C inhibit the algal cell cycle (Mühlhaus *et al.*, 2011*b*; Hemme *et al.*, 2014; Zachleder *et al.*, 2019; Ivanov *et al.*, 2021/5), alter thylakoid membranes, reduce photosynthesis, and damage respiration (Zhang *et al.*, 2022*a*) (Fig. 8). These cellular damages took place quickly, within 4 h of heat at 40°C with constant acetate supply (Zhang *et al.*, 2022*a*). However, 40°C-treated cells grew bigger and gained more biomass with constant acetate supply than without in the short-term (24-h heat) (Fig. 4B, G, D, I, L, N), although the constant acetate supply could not prevent ultimate cell death with 40°C-heat longer than 2-days (Fig. 6). The death of Chlamydomonas cultures was

555 also reported at 39°C for 33 h in photoautotrophic medium without acetate (Zachleder *et*
556 *al.*, 2019; Ivanov *et al.*, 2021/5). Thus, constant heating at 40°C is lethal for
557 Chlamydomonas cells independent of carbon availability.
558
559 Transcripts/proteins of many genes involved in carbon metabolism, e.g., acetate
560 uptake/assimilation, glyoxylate cycle and gluconeogenesis pathways, were significantly
561 down-regulated during 24-h heat of 40°C (Fig. 2F, G) (Zhang *et al.*, 2022*a*). Our previous
562 results showed that (Zhang *et al.*, 2022*a*): (1) mitochondrial activities, measured by
563 respiration rates, were particularly sensitive to 40°C heat, reduced to 50% of the pre-heat
564 level with 4 h of heat at 40°C; (2) a large fraction of transcripts related to mitochondrial
565 electron transport was down-regulated with just 30 min heat at 40°C. Most of the reducing
566 power from acetate assimilation is used in mitochondrial respiration to produce ATP
567 (Johnson and Alric, 2012, 2013). Acute high temperatures at or around 40°C cause starch
568 over-accumulation (Zachleder *et al.*, 2019; Zhang *et al.*, 2022*a*; Ivanov *et al.*, 2021/5).
569 Starch accumulation could be an electron sink to alleviate the over-reduced electron
570 transport chain in chloroplasts due to damaged photosynthesis during 40°C treatment
571 (Hemme *et al.*, 2014). The compromised mitochondrial activities and the over-
572 accumulated starch may restrict acetate uptake/assimilation and reduce photosynthesis
573 further during 40°C heat treatment. The acetate uptake was slightly lower in 40°C-treated
574 cultures than 25°C (Fig. 1D), which, together with reduced photosynthesis and respiration
575 (Zhang *et al.*, 2022*a*), may contribute to the significantly reduced algal dry biomass in
576 cultures treated with 8h-heat of 40°C than 25°C (Fig. 1C). By the end of 24-h treatment
577 without constant nutrient supply, there were comparable amount of dry biomass in
578 cultures treated with 40°C and 25°C (Fig. 1C), which could be explained by the arrested
579 cell cycle and almost eliminated energy/biomass consumption for cell division during 40°C.
580 Such an inefficient system with reduced carbon input and little energy output is not
581 sustainable, eventually killing all the algal cells by the end of 2-day heat of 40°C, even
582 with constant acetate supply (Fig. 6). As compared to the increased growth rates at 35°C
583 with constant acetate supply, the culture death during 2-day heat of 40°C may highlight
584 the importance of active carbon metabolisms in thermotolerance.
585

In summary, by using highly controlled cultivation systems and the model green alga Chlamydomonas, we revealed how the availability of organic carbon source interacted with different intensities and duration of high temperatures in photosynthetic cells. Our research revealed the overlooked effects of moderate high temperature of 35°C, which can be beneficial with constant carbon supply or detrimental with insufficient carbon supply. Our results also showed that the damaging effects of acute high temperature of 40°C is dominant and independent of carbon availability. Our research not only helps us understand heat responses in photosynthetic cells but also provides insights for high temperature effects on the production of algal biofuel/bioproducts.

Supplementary data

Table S1: Gene IDs for RT-qPCR analysis and transcript/protein heatmaps.

Acknowledgements

We would like to thank Dr. Michael Schroda for discussing the initial experimental idea under acetate depleting conditions and Dr. Trent Northen for recommending the acetate quantification assay.

Author contributions

RZ designed the experiments. MX and CB operated and maintained the algal growth in photobioreactors. MX, NZ, and CB harvested algal samples at different time points and quantified biomass. NZ and MX performed acetate quantification assay. NZ performed RT-qPCR analysis and light microscope imaging. MX and CB quantified cell density, cell size, and chlorophyll contents, and recorded $OD_{608/720}$ readings. MX and CB performed 4-day heating experiments and quantified growth rates as well as cell parameters. EMM generated the heatmaps from the published RNA-seq data. NZ, MX, CB, RZ, and EMM prepared the figures. RZ wrote the manuscript. RZ, EMM, and CB revised the manuscript.

Conflict of interest

No conflict of interest declared.

Funding statement

This work was supported by the start-up funding from the Donald Danforth Plant Science Center (DDPSC) and the DOE Biological & Environmental Research (BER) grant (DE-SC0020400) to RZ. EMM was supported by the William H. Danforth Fellowship in Plant Sciences and the DDPSC start-up funding (to RZ).

Data availability

All data supporting the findings of this study are available within the paper and within its supplementary materials published online.

References

Anderson CM, Mattoon EM, Zhang N, *et al.* 2021. High light and temperature reduce photosynthetic efficiency through different mechanisms in the C4 model Setaria viridis. Communications Biology **4**, 1092.

Aprile A, Havlickova L, Panna R, *et al.* 2013. Different stress responsive strategies to drought and heat in two durum wheat cultivars with contrasting water use efficiency. BMC genomics **14**, 821.

Baker NR, Harbinson J, Kramer DM. 2007. Determining the limitations and regulation of photosynthetic energy transduction in leaves. Plant, cell & environment **30**, 1107–1125.

Balfagón D, Sengupta S, Gómez-Cadenas A, Fritschi FB, Azad RK, Mittler R, Zandalinas SI. 2019. Jasmonic acid Is required for plant acclimation to a combination of high light and heat stress. Plant physiology **181**, 1668–1682.

Baud S, Wuillème S, Dubreucq B, de Almeida A, Vuagnat C, Lepiniec L, Miquel M, Rochat C. 2007. Function of plastidial pyruvate kinases in seeds of Arabidopsis thaliana. The Plant journal: for cell and molecular biology **52**, 405–419.

Bourgine B, Guihur A. 2021. Heat Shock Signaling in Land Plants: From Plasma Membrane Sensing to the Transcription of Small Heat Shock Proteins. Frontiers in plant science **12**, 710801.

Chapman S, Paget C, Johnson G, Schwartz J-M. 2015. Flux balance analysis reveals acetate metabolism modulates cyclic electron flow and alternative glycolytic pathways in Chlamydomonas reinhardtii. Frontiers in plant science **6**.

Chew SY, Chee WJY, Than LTL. 2019. The glyoxylate cycle and alternative carbon metabolism as metabolic adaptation strategies of Candida glabrata: perspectives from Candida albicans and Saccharomyces cerevisiae. Journal of Biomedical Science **26**.

Chioccioli M, Hankamer B, Ross IL. 2014. Flow Cytometry Pulse Width Data Enables Rapid and Sensitive Estimation of Biomass Dry Weight in the Microalgae Chlamydomonas reinhardtii and Chlorella vulgaris. PLoS ONE **9**, e97269.

Crozet P, Navarro FJ, Willmund F, *et al.* 2018. Birth of a photosynthetic chassis: A MoClo toolkit enabling synthetic biology in the microalga *Chlamydomonas reinhardtii*. ACS synthetic biology **7**, 2074–2086.

Delorge I, Janiak M, Carpentier S, Van Dijck P. 2014. Fine tuning of trehalose biosynthesis and hydrolysis as novel tools for the generation of abiotic stress tolerant plants. Frontiers in plant science **5**.

Dhokane D, Bhadra B, Dasgupta S. 2020. CRISPR based targeted genome editing of *Chlamydomonas reinhardtii* using programmed Cas9-gRNA ribonucleoprotein. Molecular biology reports **47**, 8747–8755.

van Dongen JT, Gupta KJ, Ramírez-Aguilar SJ, Araújo WL, Nunes-Nesi A, Fernie AR. 2011. Regulation of respiration in plants: a role for alternative metabolic pathways. Journal of plant physiology **168**, 1434–1443.

El-Sheekh MM, Gheda SF, El-Sayed AE-KB, Abo Shady AM, El-Sheikh ME, Schagerl M. 2019. Outdoor cultivation of the green microalga Chlorella vulgaris under stress conditions as a feedstock for biofuel. Environmental science and pollution research international **26**, 18520–18532.

Emrich-Mills TZ, Yates G, Barrett J, *et al.* 2021. A recombineering pipeline to clone large and complex genes in Chlamydomonas. The Plant Cell **33**, 1161–1181.

Erickson E, Wakao S, Niyogi KK. 2015. Light stress and photoprotection in *Chlamydomonas reinhardtii*. The Plant journal: for cell and molecular biology **82**, 449–465.

Fauser F, Vilarrasa-Blasi J, Onishi M, *et al.* 2022. Systematic characterization of gene function in the photosynthetic alga Chlamydomonas reinhardtii. Nature genetics **54**, 705–714.

Gao F, Han X, Wu J, Zheng S, Shang Z, Sun D, Zhou R, Li B. 2012. A heat-activated calcium-permeable channel - Arabidopsis cyclic nucleotide-gated ion channel 6 - is involved in heat shock responses. The Plant Journal **70**, 1056–1069.

Gil K-E, Park C-M. 2019. Thermal adaptation and plasticity of the plant circadian clock. The New phytologist **221**, 1215–1229.

Greiner A, Kelterborn S, Evers H, Kreimer G, Sizova I, Hegemann P. 2017. Targeting of photoreceptor genes in *Chlamydomonas reinhardtii* via zinc-finger nucleases and CRISPR/Cas9. The Plant cell **29**, 2498–2518.

Guo M, Liu J-H, Ma X, Luo D-X, Gong Z-H, Lu M-H. 2016. The Plant Heat Stress Transcription Factors (HSFs): Structure, Regulation, and Function in Response to Abiotic Stresses. Frontiers in plant science **7**, 114.

Han S-H, Kim JY, Lee J-H, Park C-M. 2021. Safeguarding genome integrity under heat stress in plants. Journal of experimental botany.

Heifetz PB, Förster B, Osmond CB, Giles LJ, Boynton JE. 2000. Effects of acetate on facultative autotrophy in Chlamydomonas reinhardtii assessed by photosynthetic measurements and stable isotope analyses. Plant physiology **122**, 1439–1445.

Hellemans J, Mortier G, De Paepe A, Speleman F, Vandesompele J. 2007. QBase relative quantification framework and software for management and automated analysis of real-time quantitative PCR data. Genome biology **8**, R19.

Hemme D, Veyel D, Mühlhaus T, *et al.* 2014. Systems-wide analysis of acclimation responses to long-term heat stress and recovery in the photosynthetic model organism *Chlamydomonas reinhardtii*. The Plant cell **26**, 4270–4297.

Iliev D, Voytsekh O, Schmidt E-M, Fiedler M, Nykytenko A, Mittag M. 2006. A heteromeric RNA-binding protein is involved in maintaining acrophase and period of the circadian clock. Plant physiology **142**, 797–806.

Ivanov IN, Zachleder V, Vítová M, Barbosa MJ, Bišová K. 2021/5. Starch production in *Chlamydomonas reinhardtii* through supraoptimal temperature in a pilot-scale photobioreactor. Cells **10**, 1084.

Janni M, Gullì M, Maestri E, Marmiroli M, Valliyodan B, Nguyen HT, Marmiroli N. 2020. Molecular and genetic bases of heat stress responses in crop plants and breeding for increased resilience and productivity. Journal of experimental botany **71**, 3780–3802.

Ji S, Siegel A, Shan S-O, Grimm B, Wang P. 2021. Chloroplast SRP43 autonomously protects chlorophyll biosynthesis proteins against heat shock. Nature plants **7**, 1420–1432.

Johnson GN. 2011. Physiology of PSI cyclic electron transport in higher plants. Biochimica et Biophysica Acta (BBA) - Bioenergetics **1807**, 384–389.

Johnson X, Alric J. 2012. Interaction between starch breakdown, acetate assimilation, and photosynthetic cyclic electron flow in *Chlamydomonas reinhardtii*. The Journal of biological chemistry **287**, 26445–26452.

Johnson X, Alric J. 2013. Central carbon metabolism and electron transport in *Chlamydomonas reinhardtii*: metabolic constraints for carbon partitioning between oil and starch. Eukaryotic cell **12**, 776–793.

Karpowicz SJ, Prochnik SE, Grossman AR, Merchant SS. 2011. The GreenCut2 resource, a phylogenomically derived inventory of proteins specific to the plant lineage. The Journal of biological chemistry **286**, 21427–21439.

Kim S-C, Guo L, Wang X. 2020. Nuclear moonlighting of cytosolic glyceraldehyde-3-phosphate dehydrogenase regulates Arabidopsis response to heat stress. Nature communications **11**, 3439.

Koley S, Chu KL, Mukherjee T, Morley SA, Klebanovych A, Czymmek KJ, Allen DK. 2022. Metabolic synergy in Camelina reproductive tissues for seed development. Science advances **8**, eabo7683.

Kropat J, Hong-Hermesdorf A, Casero D, Ent P, Castruita M, Pellegrini M, Merchant SS, Malasarn D. 2011. A revised mineral nutrient supplement increases biomass and growth rate in Chlamydomonas reinhardtii. The Plant journal: for cell and molecular biology **66**, 770–780.

Kusakina J, Gould PD, Hall A. 2014. A fast circadian clock at high temperatures is a conserved feature across Arabidopsis accessions and likely to be important for vegetative yield. Plant, cell & environment **37**, 327–340.

Li X, Fauser F, Jinkerson RE, *et al.* 2019. A genome-wide algal mutant library and functional screen identifies genes required for eukaryotic photosynthesis. Nature genetics **51**, 627–635.

Li X, Lawas LMF, Malo R, *et al.* 2015. Metabolic and transcriptomic signatures of rice floral organs reveal sugar starvation as a factor in reproductive failure under heat and drought stress. Plant, cell & environment **38**, 2171–2192.

Li X, Zhang R, Patena W, *et al.* 2016. An indexed, mapped mutant library enables reverse genetics studies of biological processes in *Chlamydomonas reinhardtii*. The Plant cell **28**, 367–387.

Livak KJ, Schmittgen TD. 2001. Analysis of relative gene expression data using real-time quantitative PCR and the 2(-Delta Delta C(T)) Method. Methods **25**, 402–408.

Lucker B, Kramer DM. 2013. Regulation of cyclic electron flow in *Chlamydomonas reinhardtii* under fluctuating carbon availability. Photosynthesis research **117**, 449–459.

Mata TM, Martins AA, Caetano NS. 2010. Microalgae for biodiesel production and other applications: A review. Renewable and Sustainable Energy Reviews **14**, 217–232.

Mathimani T, Pugazhendhi A. 2019. Utilization of algae for biofuel, bio-products and bio-remediation. Biocatalysis and agricultural biotechnology **17**, 326–330.

Mattoon EM, McHargue W, Bailey CE, *et al.* 2022. High-throughput Identification of Novel Heat Tolerance Genes via Genome-wide Pooled Mutant Screens in the Model Green Alga Chlamydomonas reinhardtii. bioRxiv, 2022.07.13.499508.

Merchant SS, Prochnik SE, Vallon O, *et al.* 2007. The *Chlamydomonas* genome reveals the evolution of key animal and plant functions. Science **318**, 245–250.

Minagawa J, Tokutsu R. 2015. Dynamic regulation of photosynthesis in *Chlamydomonas reinhardtii*. The Plant journal: for cell and molecular biology **82**, 413–428.

Mittler R, Finka A, Goloubinoff P. 2012. How do plants feel the heat? Trends in biochemical sciences **37**, 118–125.

Mody T, Bonnot T, Nagel DH. 2020. Interaction between the Circadian Clock and Regulators of Heat Stress Responses in Plants. Genes **11**.

Mühlhaus T, Weiss J, Hemme D, Sommer F, Schroda M. 2011*a*. Quantitative Shotgun Proteomics Using a Uniform 15N-Labeled Standard to Monitor Proteome Dynamics in Time Course Experiments Reveals New Insights into the Heat Stress Response of Chlamydomonas reinhardtii. Molecular & Cellular Proteomics **10**, M110.004739.

Mühlhaus T, Weiss J, Hemme D, Sommer F, Schroda M. 2011*b*. Quantitative shotgun proteomics using a uniform ^{15}N-labeled standard to monitor proteome dynamics in time course experiments reveals new insights into the heat stress response of *Chlamydomonas reinhardtii*. Molecular & cellular proteomics: MCP **10**, M110.004739.

Munekage Y, Hashimoto M, Miyake C, Tomizawa K-I, Endo T, Tasaka M, Shikanai T. 2004. Cyclic electron flow around photosystem I is essential for photosynthesis. Nature **429**, 579–582.

Murata N, Nishiyama Y. 2018. ATP is a driving force in the repair of photosystem II during photoinhibition. Plant, cell & environment **41**, 285–299.

Niemeyer J, Scheuring D, Oestreicher J, Morgan B, Schroda M. 2021. Real-time monitoring of subcellular H2O2 distribution in *Chlamydomonas reinhardtii*. The Plant cell.

Olas JJ, Apelt F, Annunziata MG, John S, Richard SI, Gupta S, Kragler F, Balazadeh S, Mueller-Roeber B. 2021. Primary carbohydrate metabolism genes participate in heat-stress memory at the shoot apical meristem of Arabidopsis thaliana. Molecular plant **14**, 1508–1524.

Ortiz-Bobea A, Wang H, Carrillo CM, Ault TR. 2019. Unpacking the climatic drivers of US agricultural yields. Environmental research letters: ERL [Web site] **14**, 064003.

Plancke C, Vigeolas H, Höhner R, *et al.* 2014. Lack of isocitrate lyase in *Chlamydomonas* leads to changes in carbon metabolism and in the response to oxidative stress under mixotrophic growth. The Plant journal: for cell and molecular biology **77**, 404–417.

Porra RJ, Thompson WA, Kriedemann PE. 1989. Determination of accurate extinction coefficients and simultaneous equations for assaying chlorophylls a and b extracted with

four different solvents: verification of the concentration of chlorophyll standards by atomic absorption spectroscopy. Biochimica et Biophysica Acta (BBA) - Bioenergetics **975**, 384–394.

Pospíšil P. 2016. Production of reactive oxygen species by photosystem II as a response to light and temperature stress. Frontiers in plant science **7**, 1950.

Pröschold T, Harris EH, Coleman AW. 2005. Portrait of a species: *Chlamydomonas reinhardtii*. Genetics **170**, 1601–1610.

Qin-Di D, Gui-Hua J, Xiu-Neng W, Zun-Guang M, Qing-Yong P, Shiyun C, Yu-Jian M, Shuang-Xi Z, Yong-Xiang H, Yu L. 2021. High temperature-mediated disturbance of carbohydrate metabolism and gene expressional regulation in rice: a review. Plant signaling & behavior **16**, 1862564.

Remans T, Keunen E, Bex GJ, Smeets K, Vangronsveld J, Cuypers A. 2014. Reliable gene expression analysis by reverse transcription-quantitative PCR: reporting and minimizing the uncertainty in data accuracy. The Plant cell **26**, 3829–3837.

Roach T, Sedoud A, Krieger-Liszkay A. 2013. Acetate in mixotrophic growth medium affects photosystem II in Chlamydomonas reinhardtii and protects against photoinhibition. Biochimica et Biophysica Acta (BBA) - Bioenergetics **1827**, 1183–1190.

Rochaix J-D. 2014. Regulation and dynamics of the light-harvesting system. Annual review of plant biology **65**, 287–309.

Rollins JA, Habte E, Templer SE, Colby T, Schmidt J, von Korff M. 2013. Leaf proteome alterations in the context of physiological and morphological responses to drought and heat stress in barley (Hordeum vulgare L.). Journal of experimental botany **64**, 3201–3212.

Romero-Campero FJ, Perez-Hurtado I, Lucas-Reina E, Romero JM, Valverde F. 2016. ChlamyNET: a Chlamydomonas gene co-expression network reveals global properties of the transcriptome and the early setup of key co-expression patterns in the green lineage. BMC genomics **17**, 227.

Rütgers M, Muranaka LS, Schulz-Raffelt M, Thoms S, Schurig J, Willmund F, Schroda M. 2017. Not changes in membrane fluidity but proteotoxic stress triggers heat shock protein expression in *Chlamydomonas reinhardtii*. Plant, cell & environment **40**, 2987–3001.

Sager R. 1955-7. Inheritance in the green alga *Chlamydomonas reinhardtii*. Genetics **40**, 476–489.

Saidi Y, Peter M, Finka A, Cicekli C, Vigh L, Goloubinoff P. 2010. Membrane lipid composition affects plant heat sensing and modulates Ca2+-dependent heat shock response. Plant signaling & behavior **5**, 1530–1533.

Salomé PA, Merchant SS. 2021. Co-expression networks in Chlamydomonas reveal significant rhythmicity in batch cultures and empower gene function discovery. The Plant cell **33**, 1058–1082.

Sasso S, Stibor H, Mittag M, Grossman AR. 2018. From molecular manipulation of domesticated Chlamydomonas reinhardtii to survival in nature. eLife **7**, e39233.

Schloss JA. 1990. A *Chlamydomonas* gene encodes a G protein β subunit-like polypeptide. Molecular & general genetics: MGG **221**, 443–452.

Schroda M, Hemme D, Mühlhaus T. 2015. The *Chlamydomonas* heat stress response. The Plant journal: for cell and molecular biology **82**, 466–480.

Schulz-Raffelt M, Lodha M, Schroda M. 2007. Heat shock factor 1 is a key regulator of the stress response in *Chlamydomonas*. The Plant journal: for cell and molecular biology **52**, 286–295.

Scranton MA, Ostrand JT, Fields FJ, Mayfield SP. 2015. *Chlamydomonas* as a model for biofuels and bio-products production. The Plant journal: for cell and molecular biology **82**, 523–531.

Sharkey TD. 2005. Effects of moderate heat stress on photosynthesis: importance of thylakoid reactions, rubisco deactivation, reactive oxygen species, and thermotolerance provided by isoprene. Plant, cell & environment **28**, 269–277.

Sharkey TD, Zhang R. 2010. High temperature effects on electron and proton circuits of photosynthesis. Journal of integrative plant biology **52**, 712–722.

Shimogawara K, Fujiwara S, Grossman A, Usuda H. 1998. High-efficiency transformation of *Chlamydomonas reinhardtii* by electroporation. Genetics **148**, 1821–1828.

Song Z-T, Zhang L-L, Han J-J, Zhou M, Liu J-X. 2021. Histone H3K4 methyltransferases SDG25 and ATX1 maintain heat-stress gene expression during recovery in Arabidopsis. The Plant journal: for cell and molecular biology **105**, 1326–1338.

Strenkert D, Schmollinger S, Gallaher SD, *et al.* 2019. Multiomics resolution of molecular events during a day in the life of *Chlamydomonas*. Proceedings of the National Academy of Sciences of the United States of America **116**, 2374–2383.

Su Z, Tang Y, Ritchey LE, Tack DC, Zhu M, Bevilacqua PC, Assmann SM. 2018. Genome-wide RNA structurome reprogramming by acute heat shock globally regulates mRNA abundance. Proceedings of the National Academy of Sciences of the United States of America **115**, 12170–12175.

Terashima M, Specht M, Hippler M. 2011. The chloroplast proteome: a survey from the *Chlamydomonas reinhardtii* perspective with a focus on distinctive features. Current genetics **57**, 151–168.

Voß B, Meinecke L, Kurz T, Al-Babili S, Beck CF, Hess WR. 2010. Hemin and Magnesium-Protoporphyrin IX Induce Global Changes in Gene Expression in Chlamydomonas reinhardtii. Plant physiology **155**, 892–905.

Voytsekh O, Seitz SB, Iliev D, Mittag M. 2008. Both subunits of the circadian RNA-binding protein CHLAMY1 can integrate temperature information. Plant physiology **147**, 2179–2193.

Walker RP, Chen Z-H, Famiani F. 2021. Gluconeogenesis in Plants: A Key Interface between Organic Acid/Amino Acid/Lipid and Sugar Metabolism. Molecules **26**.

Wang L, Yang L, Wen X, Chen Z, Liang Q, Li J, Wang W. 2019. Rapid and high efficiency transformation of *Chlamydomonas reinhardtii* by square-wave electroporation. Bioscience reports **39**, BSR20181210.

Wulfert S, Schilasky S, Krueger S. 2020. Transcriptional and Biochemical Characterization of Cytosolic Pyruvate Kinases in Arabidopsis thaliana. Plants **9**.

Xiao L, Young EB, Grothjan JJ, Lyon S, Zhang H, He Z. 2015. Wastewater treatment and microbial communities in an integrated photo-bioelectrochemical system affected by different wastewater algal inocula. Algal Research **12**, 446–454.

Xie B, Bishop S, Stessman D, Wright D, Spalding MH, Halverson LJ. 2013. *Chlamydomonas reinhardtii* thermal tolerance enhancement mediated by a mutualistic interaction with vitamin B12-producing bacteria. The ISME journal **7**, 1544–1555.

Yamori W, Shikanai T. 2016. Physiological functions of cyclic electron transport around Photosystem I in sustaining photosynthesis and plant growth. Annual review of plant biology **67**, 81–106.

Young EB, Reed L, Berges JA. 2022. Growth parameters and responses of green algae across a gradient of phototrophic, mixotrophic and heterotrophic conditions. PeerJ **10**, e13776.

Zachleder V, Ivanov I, Vítová M, Bišová K. 2019. Cell cycle arrest by supraoptimal temperature in the alga *Chlamydomonas reinhardtii*. Cells **8**, 1237.

Zhang N, Mattoon EM, McHargue W, *et al.* 2022*a*. Systems-wide analysis revealed shared and unique responses to moderate and acute high temperatures in the green alga Chlamydomonas reinhardtii. Communications biology **5**, 460.

Zhang N, Pazouki L, Nguyen H, *et al.* 2022*b*. Comparative Phenotyping of Two Commonly Used Chlamydomonas reinhardtii Background Strains: CC-1690 (21gr) and CC-5325 (The CLiP Mutant Library Background). Plants **11**, 585.

Zhang X, Rerksiri W, Liu A, Zhou X, Xiong H, Xiang J, Chen X, Xiong X. 2013. Transcriptome profile reveals heat response mechanism at molecular and metabolic levels in rice flag leaf. Gene **530**, 185–192.

Figures

Fig. 1.

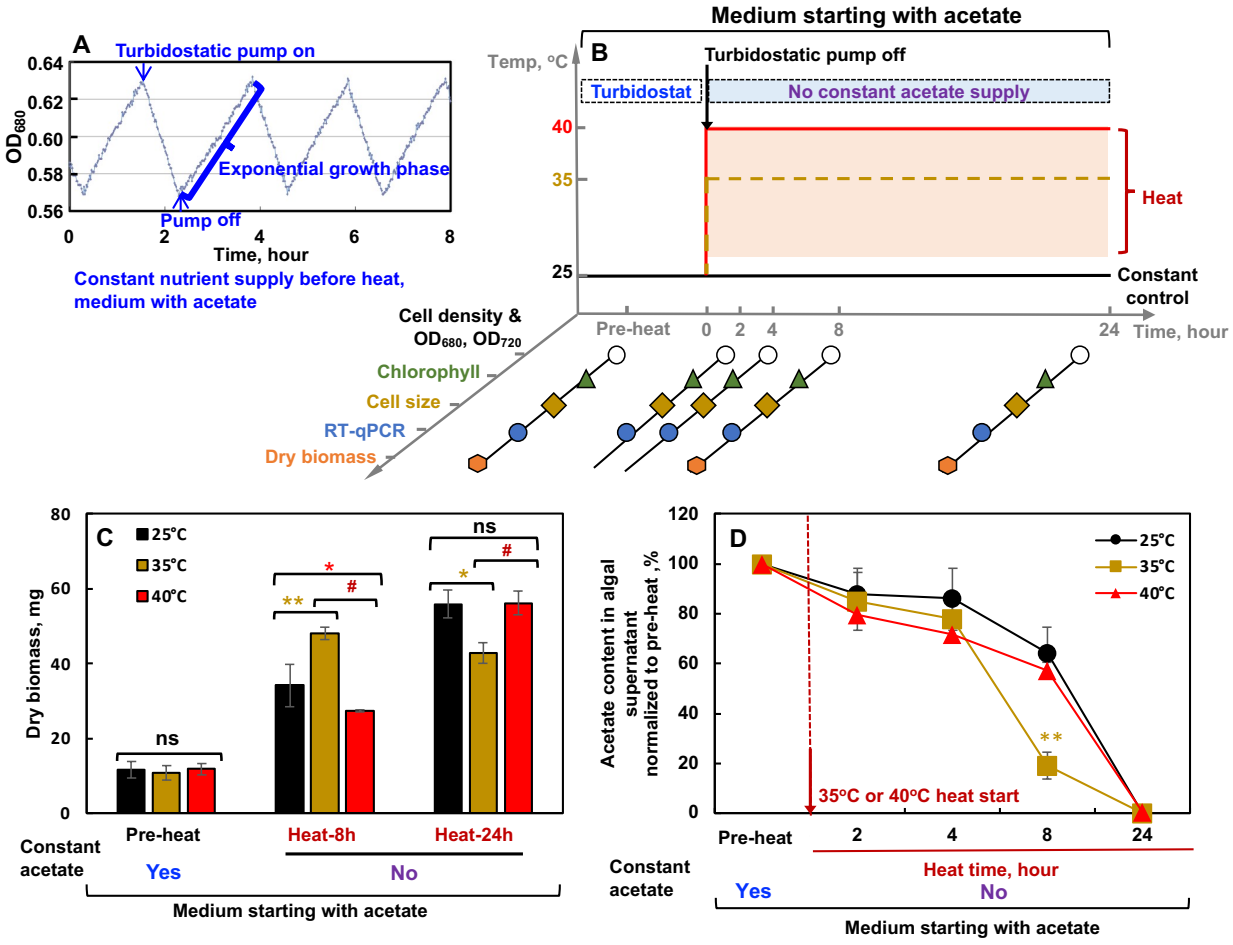

Fig. 1. Without constant acetate supply, moderate high temperature of 35°C transiently increased but then decreased Chlamydomonas biomass accumulation. **(A)** Before heat treatments, Chlamydomonas cells (CC-1690, also called *21gr*, wild-type) were grown in photobioreactors (PBRs) in Tris-acetate-phosphate (TAP) medium (acetate as an organic carbon source) with a light intensity of 100 μmol photons m^{-2} s^{-1} and constantly bubbling of air. Algal cultures were maintained turbidostatically within a small range of OD_{680} which monitors chlorophyll content (μg chlorophyll mL^{-1} cultures). When PBR cultures grew to the set maximum OD_{680}, pumps were turned on to add fresh medium and dilute the cultures to the set minimal OD_{680}, then pumps were turned off to allow for exponential growth to the maximum set OD_{680}. Figure cited from a supplementary figure of this paper (Zhang *et al.*, 2022*a*). **(B)** Experimental outline. The

PBR cultures were first maintained at 25^{o}C with constant nutrient supply using the turbidostatic mode as mentioned above. After the cultures reached steady growth (pre-heat time point), the turbidostatic pumps were turned off and the cultures were grown under the indicated temperature for 24 hours (h) without fresh medium supply (thus no constant acetate supply). Algal cultures were harvested at different time points for the indicated parameters. Each temperature treatment was conducted in an individual PBR with at least 3 replicates. **(C)** Without constant acetate supply, algal dry biomass increased with 8-h heat but decreased with 24-h heat of 35^{o}C as compared to the constant 25^{o}C. Mean ± SE, *n*=3-8 biological replicates. **(D)** Heat at 35^{o}C accelerated acetate consumption. Algal cultures were harvested at different time points and acetate content in algal supernatant was quantified using Acetate Colorimetric Assay Kit. The red dashed line marks the start of heating at 35^{o}C or 40^{o}C. **(C, D)** Statistical analyses were performed using two-tailed t-test assuming unequal variance; *, $p<0.05$; **, $p<0.01$; Not significant, ns; the colors of the asterisks match the heated condition as compared to 25^{o}C at the same time points; #, $p<0.05$, for the comparisons between 35^{o}C and 40^{o}C.

Fig. 2.

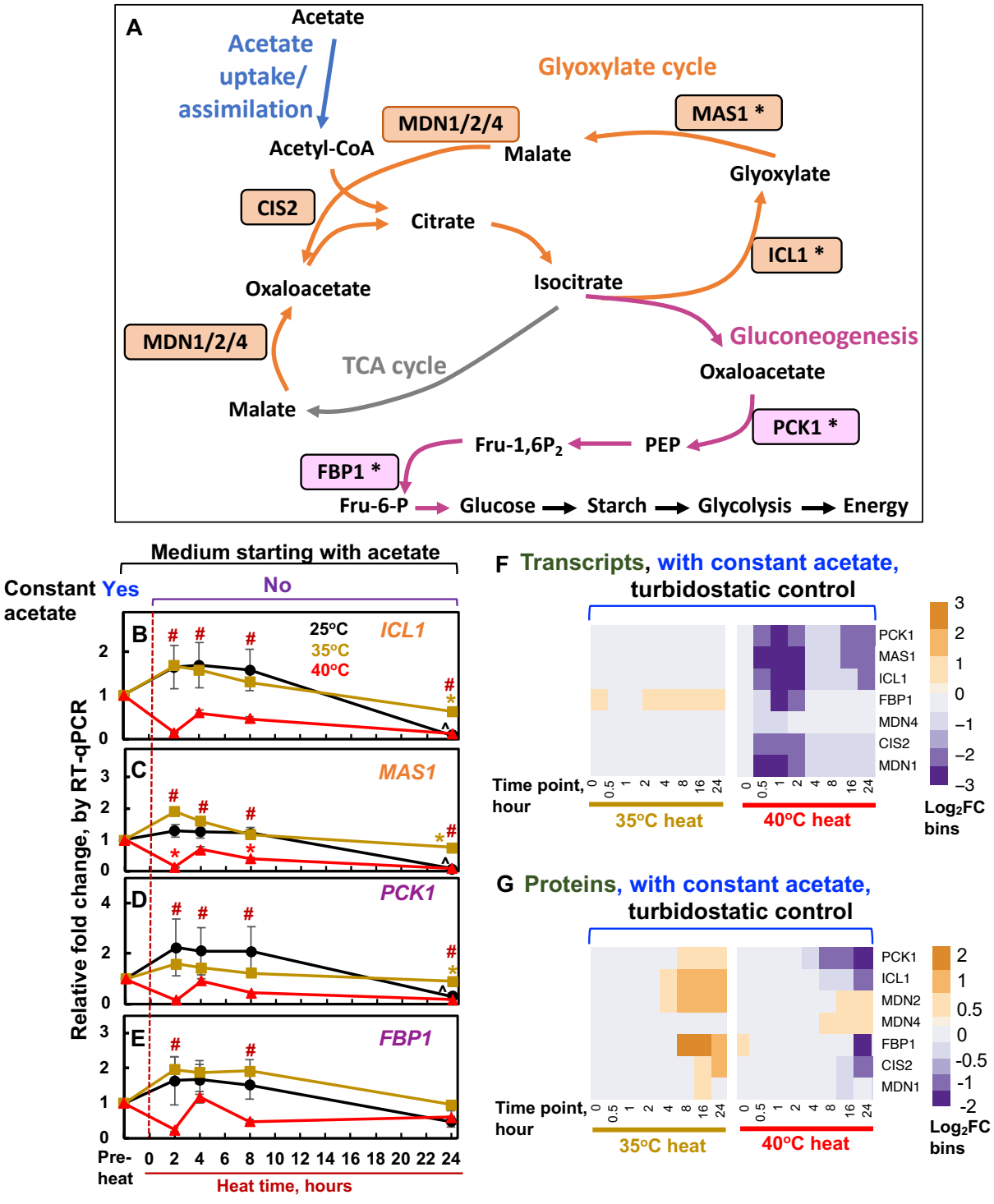

Fig. 2. The dynamic effects of 35°C on algal biomass without constant acetate supply is related to the up-regulation of glyoxylate cycle and gluconeogenesis

pathways. (A) Simplified pathways of acetate uptake/assimilation, glyoxylate cycle, and gluconeogenesis based on this paper (Johnson and Alric, 2013). Key enzymes are in boxes and those with asterisks were used for RT-qPCR analysis in panels B-E. Glyoxylate cycle key enzymes: ICL1, isocitrate lyase; MAS1, malate synthase. Gluconeogenesis key enzymes: PCK1, phosphoenolpyruvate carboxykinase; FBP1, fructose-1,6-bisphosphatase (See all gene IDs and annotations in Supplementary Table S1). PEP, phosphoenolpyruvate. Fru-6-P, fructose-6-phosphate. Fru-1,6-P_2, fructose-1,6-bisphosphate. **(B-E)** Without constant acetate supply, transcripts related to glyoxylate cycle and gluconeogenesis pathways were up-regulated at the end of 24-h heat of 35ºC but down-regulated at 24-h of 25ºC. The relative expressions were calculated from RT-qPCR results by normalizing to the reference genes *CBLP, EIF1A* and pre-heat level. Mean ± SE, *n* = 3 biological replicates. Statistical analyses were performed with two-tailed t-test assuming unequal variance; *, $p<0.05$, the colors of the asterisks match the heated condition as compared to 25ºC at the same time point; #, $p<0.05$, for the comparisons between 35ºC and 40ºC at the same time point; ^, $p<0.05$, for the comparisons between different time points at 25ºC (no constant acetate) with the pre-heat, constant-acetate condition. The algal cultivation and heat treatments were the same as in Fig. 1B. The red dashed line marks the start of heat at 35ºC (brown squares) or 40ºC (red triangles). The control culture was maintained at 25ºC (black circles). All cultures started with TAP medium, then no constant acetate supply starting with the 0-h time point. (**F, G**) The relative expression level of transcripts and proteins related to glyoxylate cycle and gluconeogenesis pathways during 35ºC or 40ºC heat treatments with constant acetate supply through turbidostatic mode. Heatmaps were plotted based on the transcriptomes and proteosomes data published in this paper (Zhang *et al.*, 2022*a*). Only annotated transcripts/proteins with significantly changed expressions in at least one time points were included in the heatmaps. FC, fold-change. Differential expression model output log_2FC values were sorted into different expression bins. Heating time points were labeled at the bottom: 0 h, reach high temperature of 35ºC or 40ºC; 0.5 h, heat at 35ºC or 40ºC for 0.5 h, similar names for other time points during heat.

Fig. 3.

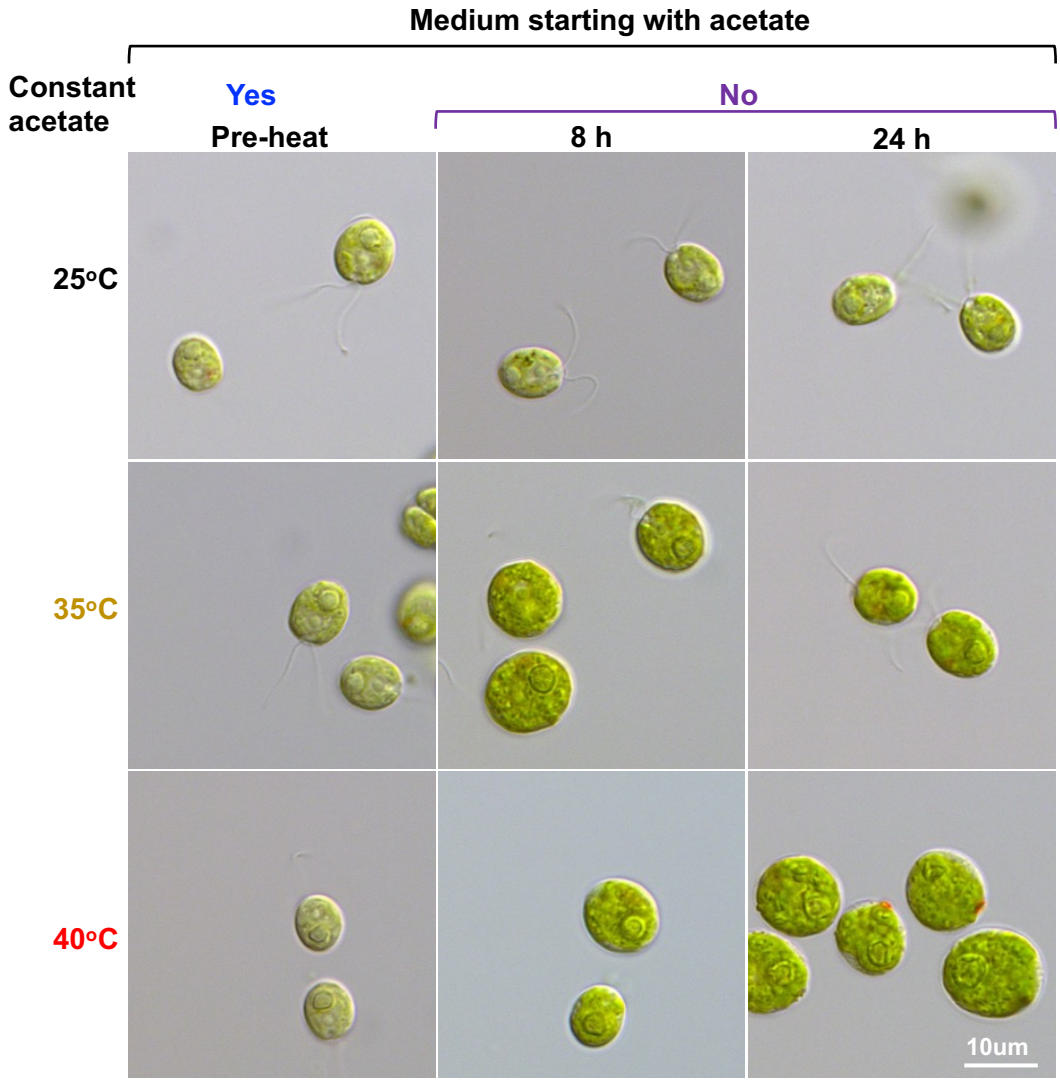

Fig. 3. Heat at 35°C transiently increased algal cell size. Light microscopic images of Chlamydomonas cells without constant acetate supply in medium starting with acetate. Images shown are representative results from at least three biological replicates. The algal cultivation and heat treatments were the same as in Fig. 1B.

Fig. 4.

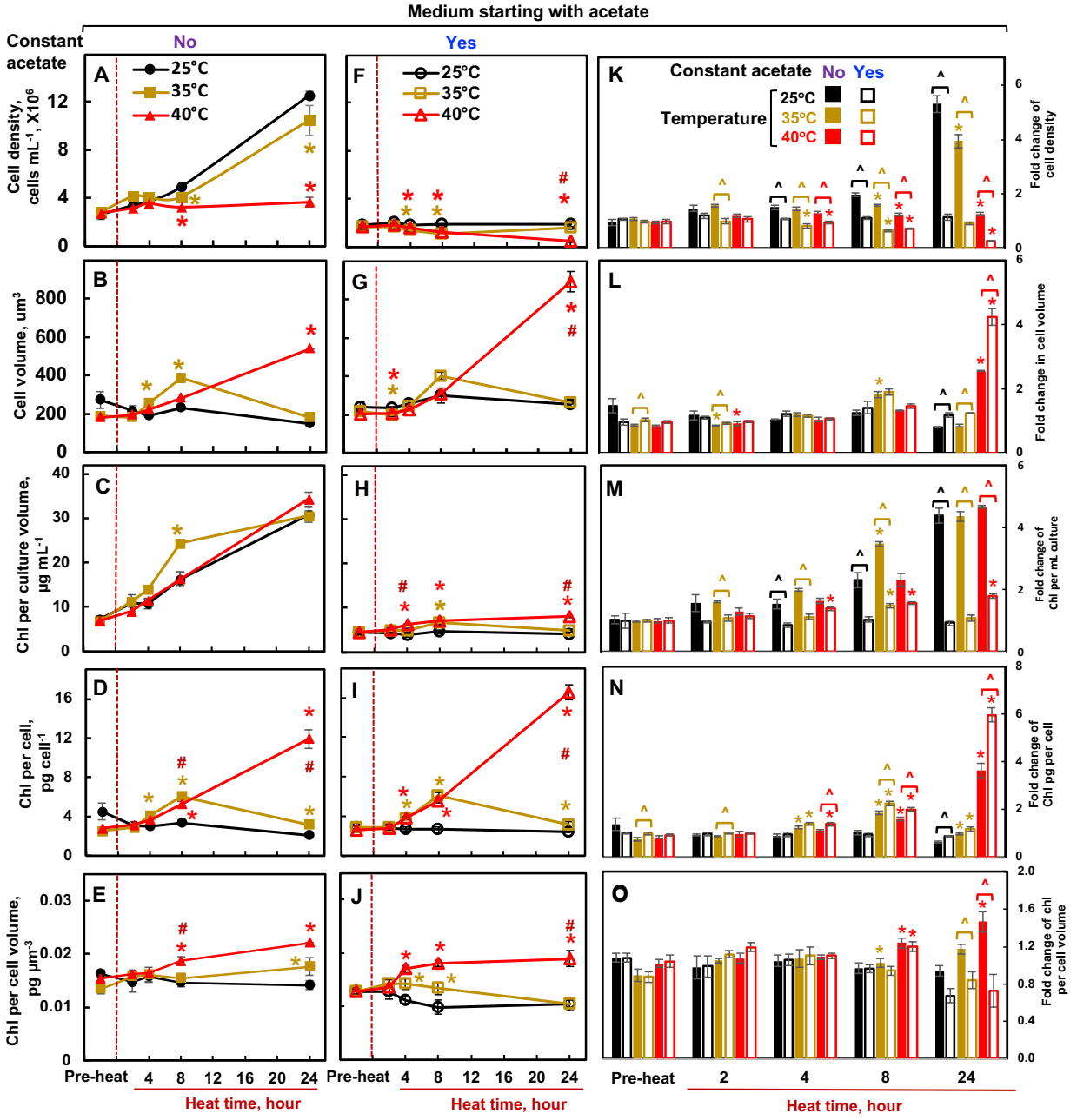

Fig. 4. Acetate availability affected algal cell physiologies during 35°C or 40°C heat in medium starting with acetate. (A-E) Cell parameters from algal cultures without constant acetate supply. The algal cultivation and heat treatments were the same as in Fig. 1B. **(F-J)** Cell parameters from algal cultures with constant acetate supply via turbidostatic mode, data plotted based on the results from this paper (Zhang *et al.*, 2022*a*). Mean ± SE, *n* = 3-7 biological replicates. (**A-J**) Two panels on the same row share the

same y axis. The red dashed line marks the start of heat. **(K-O)** Fold change of the indicated cell parameters from algal cultures without (filled bars) and with (empty bars) constant acetate supply. Statistical analyses were performed with two-tailed t-test assuming unequal variance; *, $p<0.05$, for the comparisons between 35°C or 40°C with 25°C at the same time point under the same acetate condition, the colors of the asterisks match the heat condition; #, $p<0.05$, for the comparisons between 35°C and 40°C; ^, $p<0.05$, for the comparisons between with and without constant acetate supply at the same time point. **(D-J)** Cell parameters at different time points during constant 25°C had little change, not significantly different from the pre-heat time points ($p>0.05$).

Fig. 5.

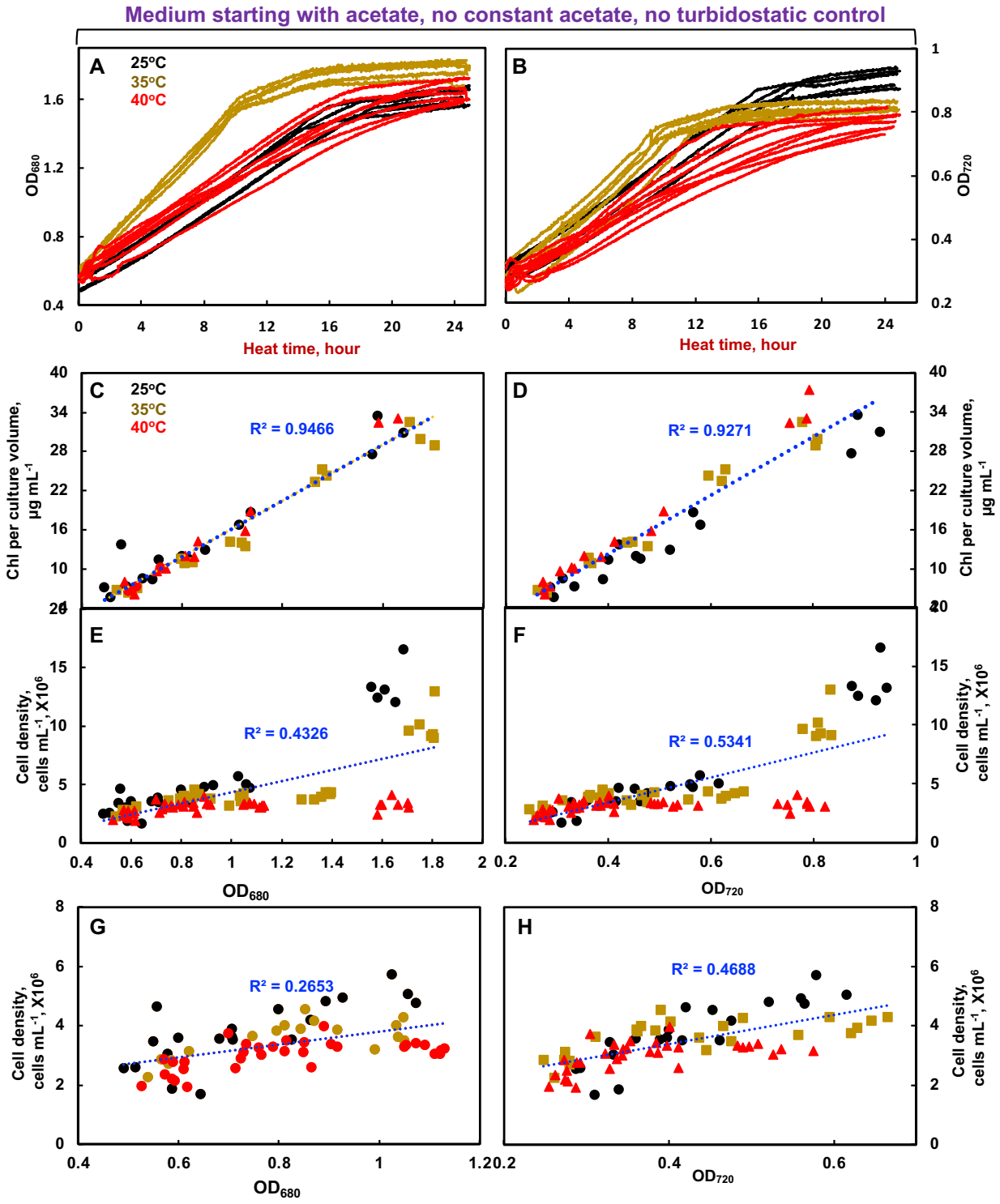

Fig. 5. OD_{680} and OD_{720} both were linearly proportional to chlorophyll contents under different temperatures and can be used to estimate algal growth rates. (A, B)

OD_{680} and OD_{720} readings in algal cultures grown in photobioreactors under different temperatures without constant acetate supply (no turbidostatic control) in medium starting with acetate. The algal cultivation and heat treatments were the same as in Fig. 1B. Lines with the same colors represent biological replicates (n= 4-8) under the same condition. **(C-F)** Chlorophyll (Chl) contents and cell densities were plotted against OD_{680} or OD_{720} readings in algal cultures with different treatments mentioned above. Dashed blue lines are linear trendlines of best fit and R-squared values are displayed. **(G, H)** The same data as in panel E-F but with smaller ranges for X values.

Fig. 6.

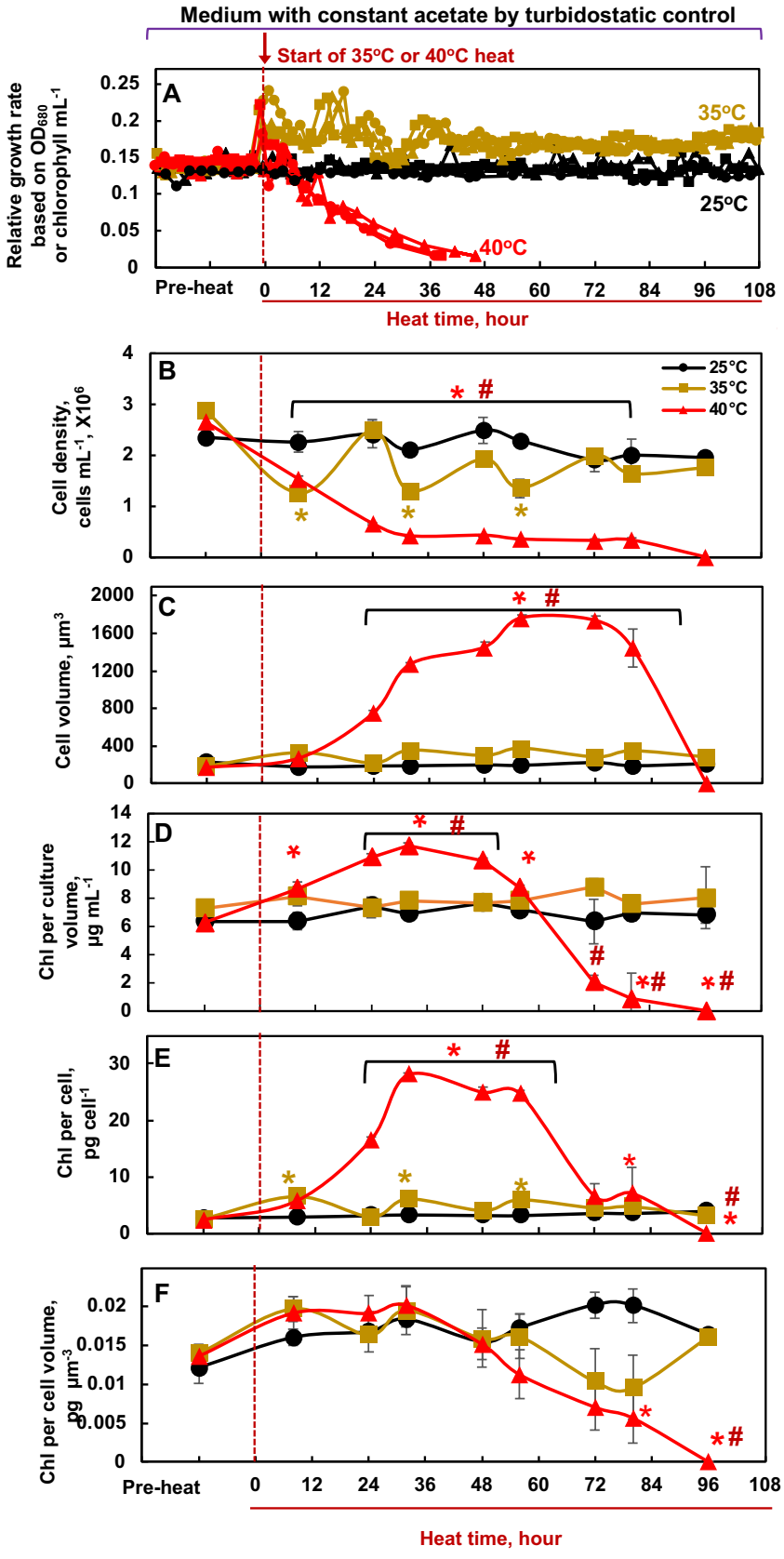
Medium with constant acetate by turbidostatic control
Start of 35°C or 40°C heat
A
35°C
25°C
40°C
Relative growth rate based on OD680 or chlorophyll mL-1
Pre-heat
Heat time, hour
B
25°C
35°C
40°C
Cell density, cells mL-1, X10^6
C
Cell volume, µm3
D
Chl per culture volume, µg mL-1
E
Chl per cell, pg cell-1
F
Chl per cell volume, pg µm-3

Fig. 6. Moderate and acute high temperatures had distinct effects on algal growth and cell parameters during 4-day heating with constant acetate supply and turbidostatic control. (A) Chlamydomonas cultures were grown in photobioreactors under turbidostatic conditions at different temperatures in acetate-containing medium. Algal cultures were first acclimated at 25ºC for 4 days before the temperature was switched to 35ºC or 40ºC or stayed at 25ºC for 4 days. The red dashed line marks the start of heat at 35ºC or 40ºC. Relative growth rates were calculated based on the cycling of OD_{680} caused by the turbidostatic control (see Fig. 1A and method for details). Each temperature treatment had 3 biological replicates in separate PBRs. **(B-F)** Cell parameters were quantified from algal cultures harvested at different time points with different treatments. Statistical analyses were performed with two-tailed t-test assuming unequal variance by comparing 35ºC or 40ºC with 25ºC at the same time point. *, $p<0.05$, the colors of the asterisks match the heated condition; #, $p<0.05$, for the comparisons between 35ºC and 40ºC. Chlorophyll, Chl.

Fig. 7.

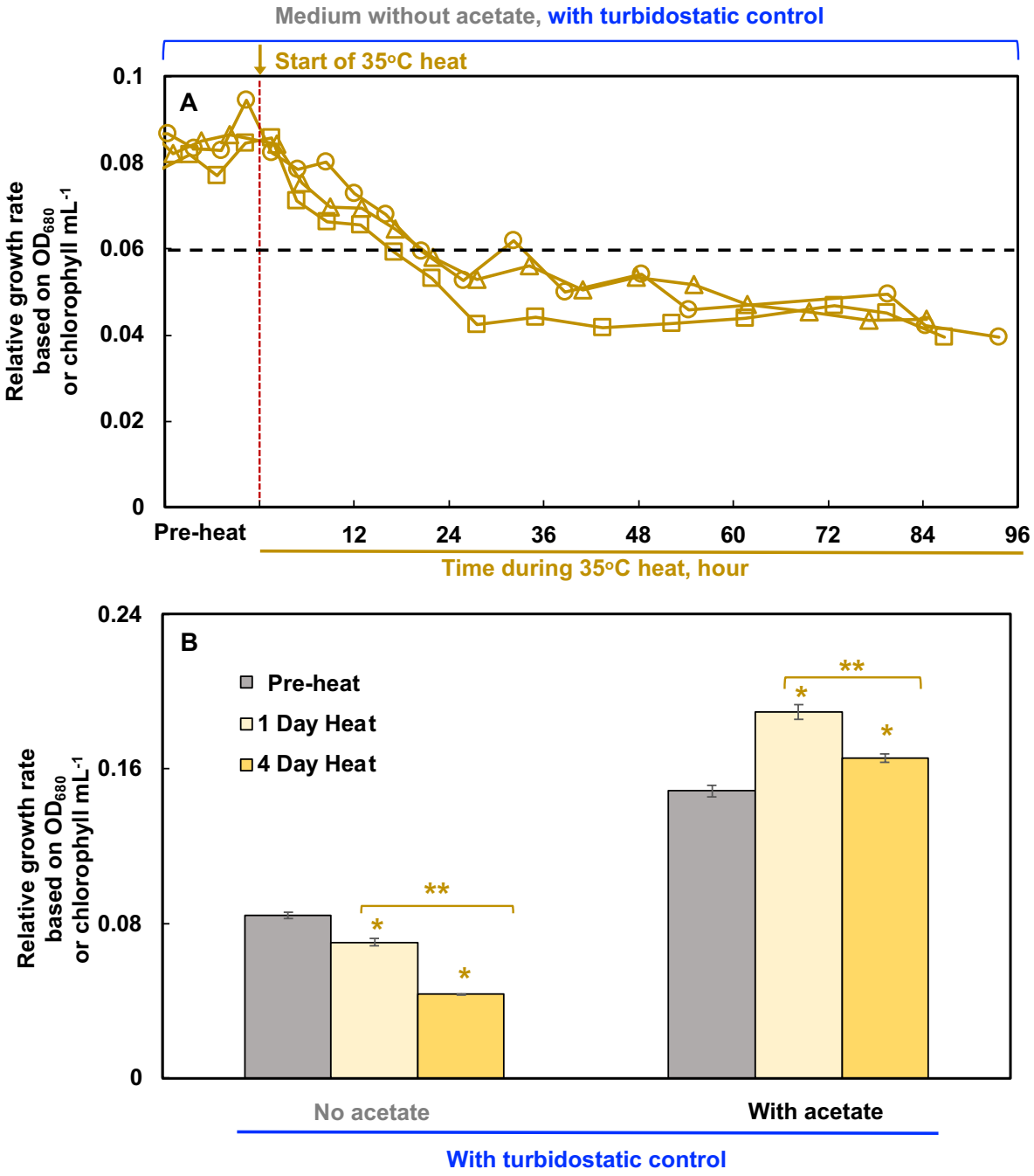

Fig. 7. Chlamydomonas cells had reduced growth during 4-day heat of 35°C with constant nutrient supply but no acetate. (**A**) Relative growth rates from algal cultures grown in photobioreactors with constant nutrient supply using the turbidostatic mode in photoautotrophic medium (Tris-phosphate, TP, no acetate). Relative growth rates were calculated based on the cycling of OD_{680} caused by the turbidostatic control (see Fig. 1A

and method for details). The red dashed line marks the start of heat at 35^{o}C. Data plots are three biological replicates. (**B**) Comparison of relative growth rates during 4-day heat of 35^{o}C using the turbidostatic mode with and without acetate. The data with constant acetate was based on the results from this paper (Zhang *et al.*, 2022*a*). Mean relative growth rates before heat, during the 1st and 4th day of heat were plotted. Mean ± SE, n = 3 biological replicates, each with 3-7 data points. Statistical analyses were performed with two-tailed t-test assuming unequal variance by comparing with pre-heat or between the 1st and 4th day of heat (under brackets); *, $p<0.05$; **, $p<0.01$.

Fig. 8.

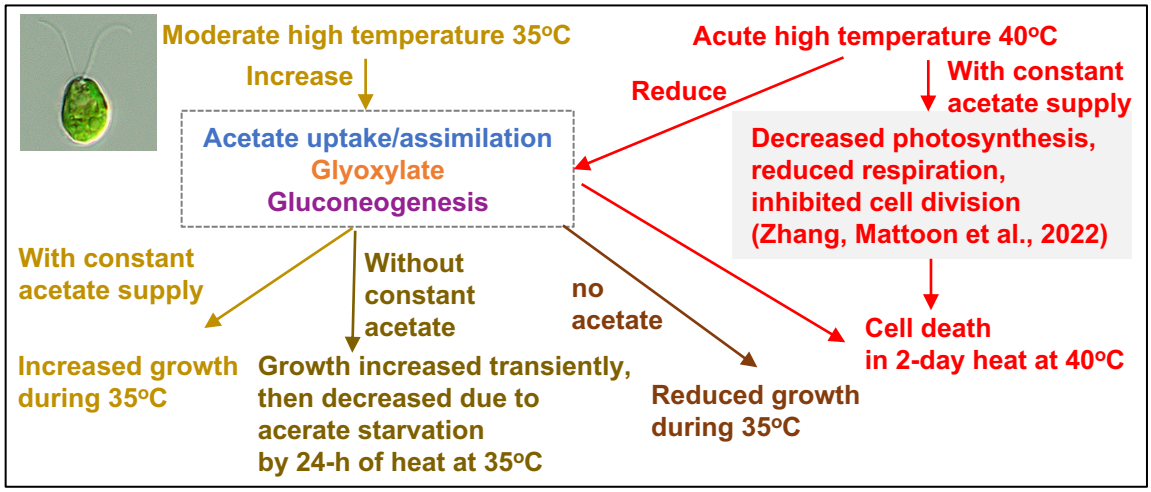

Fig. 8. A model to depict how carbon availability impacts the effect of moderate (35ºC) and acute high temperatures (40ºC) on Chlamydomonas growth. Heat of 35ºC accelerates carbon metabolisms through increased acetate uptake/assimilation, glyoxylate cycle, and gluconeogenesis pathways. With constant acetate supply, 35ºC increases algal growth. Without constant acetate supply, 35ºC increases algal growth transiently followed by decreased growth and biomass accumulation due to acetate starvation. Heat of 40ºC reduces transcripts/proteins related to acetate uptake, glyoxylate cycle, and gluconeogenesis pathways, decreases photosynthesis, reduces respiration, and inhibits cell division based on our previous results (Zhang *et al.*, 2022*a*). Thus, Chlamydomonas cells cannot survive heat of 40ºC for longer than 2-days, even with constant acetate supply.